International Journal of Mechanical and Industrial Technology ISSN 2348-7593 (Online)
Vol. 9, Issue 1, pp: (19-33), Month: April 2021 - September 2021, Available at: www.researchpublish.com

Numerical analysis of span-wise aspect ratio effect on the 2D flow stability in Lid-driven cavity using the energy gradient theory

Mapanga Mbemba Cloud Messie Rodelay, Hua-Shu Dou*

Faculty of Mechanical Engineering and Automation, Zhejiang Sci-Tech University
Xiasha Higher Education Area, Hangzhou, Zhejiang 310018, PR China,
3287399585@qq.com , cloudmessie@yahoo.co.uk

Abstract: **The two-dimensional flow characteristics in the lid- driven square cavity are simulated using the computational Fluid Dynamic (CFD). The governing equations are Navier-Stokes Equations, they are discretized with Finite Volume Method (FVM) and the software Fluent is used to calculate. A stretched quadrilateral mesh with 75000 cells was used. Various Reynolds numbers (100, 500,1000 and 2000) and aspect ratio H/L (0.5, 1, 2 and 4) in the flow characteristics is studied. Then the calculating results are compared with the numerical results in literature and the results obtained shows a good agreement. After that, the shape of vortex was investigated and the instability of the flow field was analyzed by the energy gradient theory. It has been found that the magnitude of K is proportional to the Reynolds number, the higher Reynolds number is, the bigger the K value becomes which means that the fluid become more unstable. The $K_{max}$is located at the corner region between the circulation vortices and the static walls of the square. According to energy theory the K_{max} position will lose the stability earlier than the other position. The K_{max} position change and tends to settle to the left wall of square when the Reynolds number increase. The shape of the vortex is controlled by the aspect ratio as well as the Reynolds numbers.**

Keywords: **Numerical simulation, laminar flow, lid driven cavity, energy gradient theory.**

Nomenclatures

L	[m]	length of the cavity in x direction
H	[m]	height of cavity normal direction
H/L	[-]	aspect ratio
P	[N/ m^2]	Pressure
Re	[-]	Reynolds numbers
U	[m/s]	x- component velocity
V	[m/s]	y- component velocity
K	[-]	Energy gradient

Greek Symbols

μ	[Pa. s]	fluid dynamic viscosity
ρ	[kg/m^3]	fluid density
φ		Energy dissipation function

1. INTRODUCTION

The lid driven cavity flow is the motion of the fluid inside a rectangular cavity created by constant translational velocity of one side while the other sides remain statics. Lid driven cavity flow are important in many industrial processing applications such as short dwell and flexible blade coasters. They also provide a model understanding more complex flows with closed re-circulation regions, like flow over a slit, contraction flow and roll coating flows. Cavity flows contain a full range of flow types from pure rotation near a center of re-circulation region to strong extension near edges of the lid. Fluid flow behaviors inside lid driven cavities have been the subject of extensive computational and experimental studies over the past years.

The lid-driven square cavity flow due to the simplicity of his geometry has been used as a benchmark problem for many numerical methods and the validation of Navier-Stokes codes. However, the presence of singularities at the two corners where the velocity is discontinuous makes difficult to properly evaluate the accuracy of numerical results, mainly in the neighborhood of these points. (**O. Botella and R. Peyret**).In literature, it possible to find different numerical and experimental studies on the flow in the lid-driven cavity. Here are some of them:**Botella and Peyret (1)** have used Chebyshev collocation methods of the lid driven flow. They have used subtraction method of leading terms of the asymptotic expansion of the solution of the N-S equations in the vicinity of corners, where the velocity is discontinuous, and obtained a high accurate spectral solution for the cavity flows for the Reynolds number Re<9000. They stated that their numerical solutions exhibit a periodic behavior beyond this Re.**Rubin and Khosla (2)** have used the strongly implicit numerical method with 2*2 coupled stream function-vorticity from the Navier-Stokes equations. They have obtained solutions for Reynolds number in the range of Re<3000. **Ghia et al, (3)** have later applied a multi-grid strategy to the coupled strongly implicit method developed by Rubin and Khosla (), They have presented solutions for Reynolds number as high as 10000 with meshes consisting as many as 257 *257 grid points.**Li et al (4)** have used the new version of multiple relaxation time **lattice Boltzmann method** to investigate the fluid in cavity.**Hou et al (5)** have studied the cavity flow for various Reynolds numbers using **LB-BGK model.Yang et al. (6)** investigated the flow pattern in lid-driven semi-circular cavity using **MRT model** for higher Reynolds numbers ranging from 5000 to 50000, and the result shows the stability on the **MRT** model for higher Reynolds numbers.

Therefore, the objectives of this work are to provide a CFD study of incompressible viscous laminar flow in square cavity over several arrange of Reynolds number and different aspect ratio by using FLUENT. The energy gradient theory has been used to provide the numerical analysis of the flow behavior in the lid driven. The Energy gradient theory has been proposed by Dou and Co-Authors which can be used to analyze the flow stability and turbulent transition. Recently the energy gradient theory has been successfully used to study plane Couette flow, the plane Poiseuille flow, Taylor- Couette flow, natural Convection, even in viscoelastic flow.

2. GOVERNING DIFFERENTIAL EQUATIONS

The two-dimensional flow is commonly represented by using the stream function and vorticity formulation of Navier-Stokes equations such as:

Stream function equation: $$\psi_{xx} + \psi_{yy} + \omega = 0 \quad (1)$$

Vorticity transport equation: $$\omega_{xx} + \omega_{yy} - \mathrm{Re}[(\psi_y \omega)_x - (\psi_x \omega)_y] = \mathrm{Re}\,\omega_t \quad (2)$$

Where, **Re** is Reynolds number, **x** and **y** are the Cartesian coordinates.

The fluid flow can be simulated by defining mass and momentum conservation equations. The Navier-Stokes equation are non-linear and for the lid driven cavity they are given as:

Continuity equation : $$\frac{\partial u}{\partial x} + \frac{\partial v}{\partial y} = 0 \quad (3)$$

Momentum equation x: $$\frac{\partial u}{\partial t} + u\frac{\partial u}{\partial x} + v\frac{\partial u}{\partial y} = -\frac{\partial p}{\partial y} + \frac{1}{\mathrm{Re}}\left[\frac{\partial^2 u}{\partial x^2} + \frac{\partial^2 u}{\partial y^2}\right] \quad (4)$$

Momentum equation y: $$\frac{\partial u}{\partial t} + u\frac{\partial v}{\partial x} + v\frac{\partial v}{\partial y} = -\frac{\partial p}{\partial y} + \frac{1}{\mathrm{Re}}\left[\frac{\partial^2 v}{\partial x^2} + \frac{\partial^2 v}{\partial y^2}\right] \quad (5)$$

2.1 Boundary condition:

The upper wall moves to the right with constant velocity u (u=1 and v=0), and no slip velocity condition is applied at the static walls (u=0 and v=0). The bottom boundary of the domain is considered as wall.

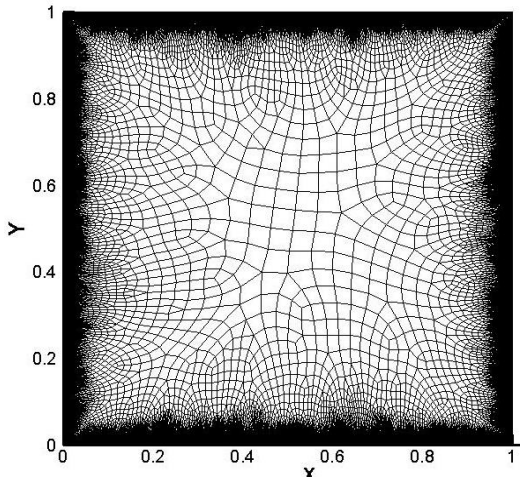

Fig 1. Computational mesh for aspect ratio 1 (75000 cells).

3. NUMERICAL MODEL AND ENERGY GRADIENT THEORY

3.1 Numerical model

A finite volume method has been employed using the FLUENT to solve the governing equations subjects to specified boundary conditions. The convective term in the governing equations is discretized with the second order upwind scheme, while the diffusion term is approximated with the central scheme. The discretized equations are solved using Semi-Implicit Method for Pressure Linked-Equations (SIMPLE) method. We define drag coefficient C_p as:

$$C_p = \frac{2(p-p_\infty)}{\rho U_\infty^2 A} \qquad (6)$$

$\boldsymbol{U}_\infty$: lid velocity, $\boldsymbol{p}_\infty$: pressure of the stream, $\boldsymbol{A}$: surface area

Validation of results

In order to valid the employed method on this paper, comparison of **U** velocity profile along horizontal lines passing through the center of cavity is made between these simulations with data from the literature Ghia et Al. Also, an extensive mesh sensitivity **(65*65, 129*129, 251*251**) has been carried to investigate that our computed results are grid dependent. **Fig:2.** There is a good quantitative agreement between this literature data and our numerical results. Indeed, the maximum relative difference between our results and those of Ghia et al does not exceed 3%.

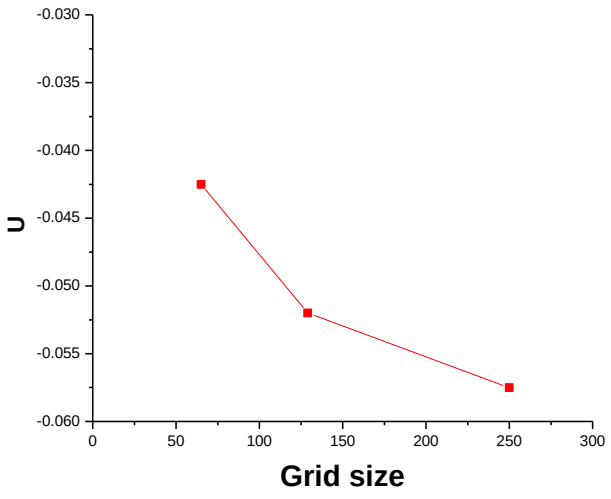

Fig 2. Grid depend tests (65*65, 129*129, 251*251) for X=$^1/_2$ at Reynolds Number 1000.

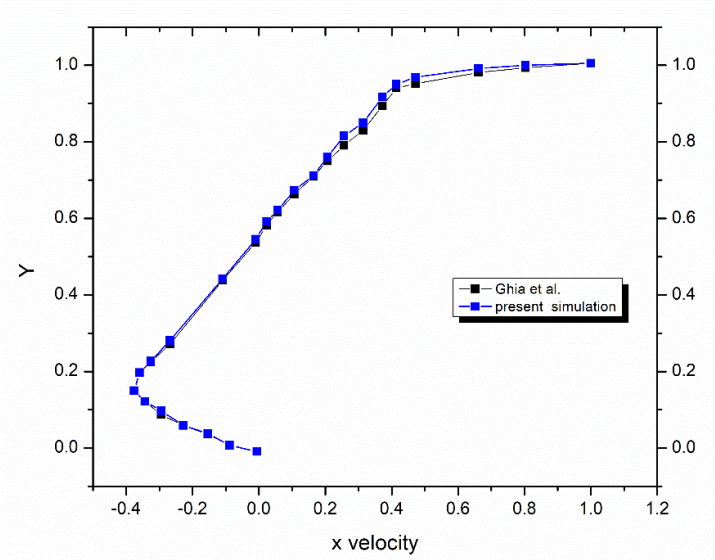

Fig 3. Comparison of U-velocity profiles along horizontal line passing through the geometric center of the cavity at X=1/2

3.2 Energy gradient theory

The energy gradient method is based on Newtonians mechanics to investigate the flow stability, it has been proposed by **Dou and Co-author** (2006). The theory has been used to determine the flow stability and the turbulent transition in different and good agreement with experiment has been obtained. This theory shows that for a giving parallel base flow, the fluid particle moves ahead with oscillation when it subjected to the interference.

The fluid gains the energy ΔE leading to amplification of the interference, and it also loose the energy ΔH in stream-wise direction which tends to absorb the disturbance and keep the original laminar flow. The transition to turbulence depends on the relative magnitude of the two roles of energy gradient amplification and viscous friction damping under given interference. When the ratio reaches a critical value the flow instability may be more imposing. The determining criterion of the instability can be written as:

$$F = \frac{\Delta E}{\Delta H} = \frac{\partial E 2A}{\partial n \pi} \Big/ \frac{\partial E 2A}{\partial n \pi}$$

$$= \frac{2}{\pi^2} k \frac{A\omega_d}{u} = \frac{2}{\pi^2} k \frac{u_m^{'}}{u} \langle \text{Constant} \qquad (7)$$

$$K = \frac{V \frac{\partial E}{\partial n}}{V \frac{\partial W}{\partial s}} = \frac{V \frac{\partial E}{\partial n}}{V \frac{\partial E}{\partial s} + \varphi} \qquad (8)$$

F is a function of coordinates which expresses the ratio of energy gained in a half period by the particle and the energy lost due to the viscosity in half period.

K is a dimensionless variable function; it represents the ratio of transversal energy gradient and the rate of energy lost along streamline.

$E = p + \frac{1}{2}\rho v^2$ is a total mechanic energy: p is a static pressure of flow; ρ is a density of flow.

Moreover W, s and n are the work done by the viscous shear stress, the steam wise direction, transversal direction along the streamline, respectively. Additional φ is the energy dissipation function caused by the viscosity and it can be written as:

$$\varphi = 2\mu D^2 = 2\mu\left[\frac{1}{2}\left(\nabla V + \nabla V^T\right)\right]^2 \qquad (9)$$

Here, μ is dynamic coefficient, D is the strain rate tensor.

Nowadays the theory has been successfully applied Taylor-Couette flow; plane Couette; plane Poiseuille and pipe Poiseuille flow and it found that the results show a good agreement with the experiment.

based on energy gradient theory, the instability would occur firstly at the location of the highest value of K., called K_{max} .

Equation can be written as:

$$K = \frac{\partial E / \partial n}{\partial H / \partial s} = \frac{\frac{\partial(p + \frac{1}{2}\rho U^2)}{\partial n}}{\frac{\partial(p + \frac{1}{2}\rho U^2)}{\partial s}} \qquad (10)$$

$$= \frac{\rho(\vec{U} \times \omega) \bullet \frac{d\vec{n}}{|d\vec{n}|} + (\mu \nabla^2 \vec{U}) \bullet \frac{d\vec{n}}{|d\vec{n}|}}{\rho(\vec{U} \times \omega) \bullet \frac{d\vec{s}}{|d\vec{s}|} + (\mu \nabla^2 \vec{U}) \bullet \frac{d\vec{s}}{|d\vec{s}|}} \qquad (11)$$

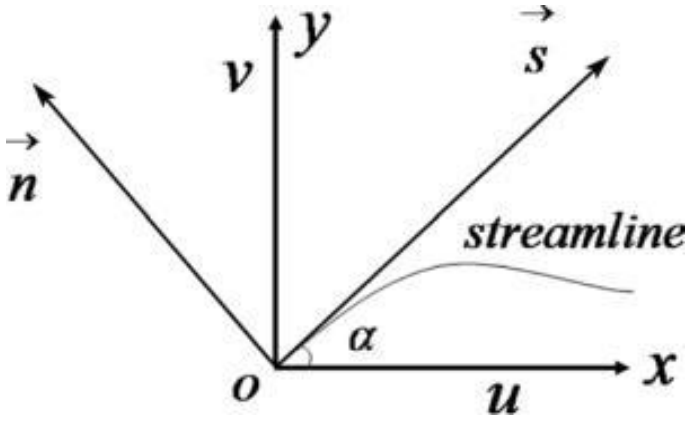

Fig 4: geometric relationship of physical quantities

4. SIMULATION RESULTS AND DISCUSSION

Mean flow:

Here is the distribution of the total velocity and the vortex at three different values of Reynolds number (Re=100,Re=500 and Re=1000) with different aspect ratio (H/L=0.5,H/L=1,H/L=2H/L=4).We observe the typical behavior of the configuration flow known by many authors in the literature.In addition to the primary vortex involved in the center of the domain, a significant growth of secondary vortices increases exponentially with increasing Reynolds number and affects the localization centers of these vortices.

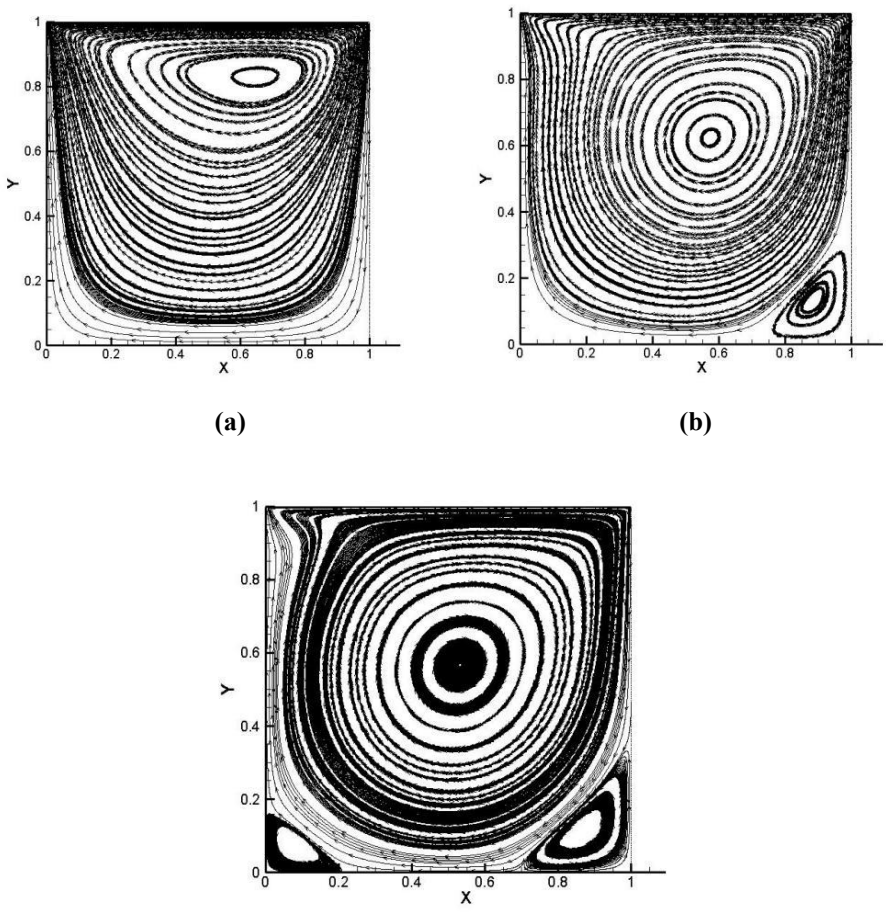

(a) (b)

(c)

Fig 5. Streamline of velocity for H/L=1, (a) Re=100 (b) Re=500 (c) Re=1000

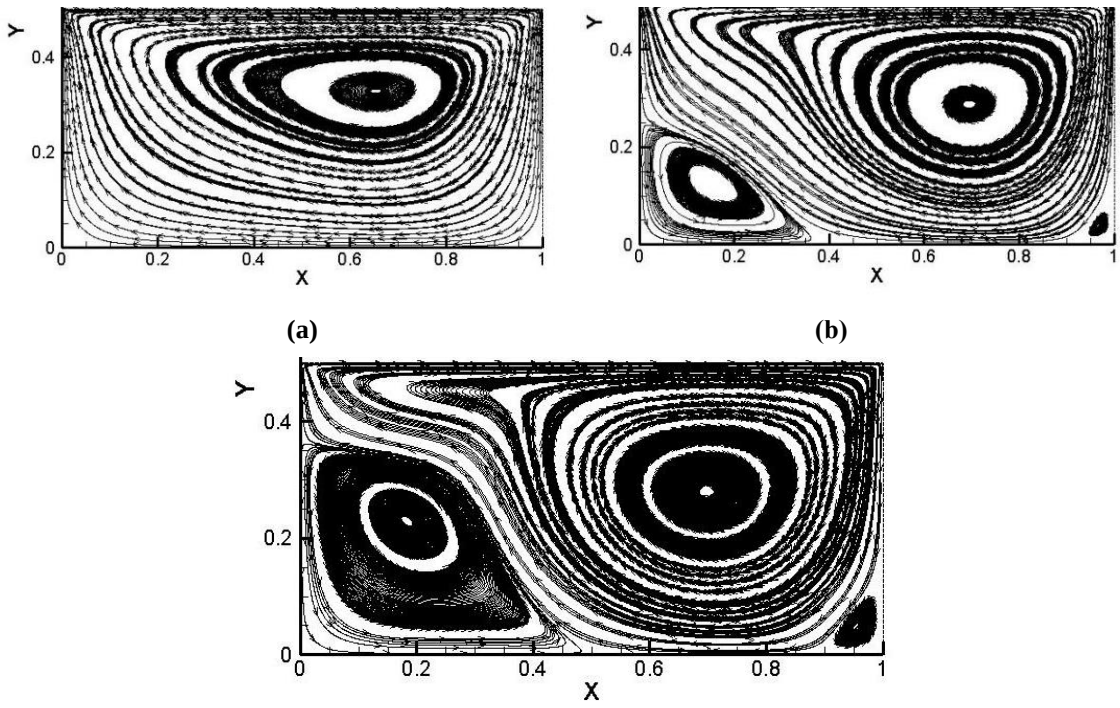

(a) (b)

(c)

Fig 6. Streamline of for H/L=1/2, (a) Re=100 (b)Re=500 (c)Re=1000

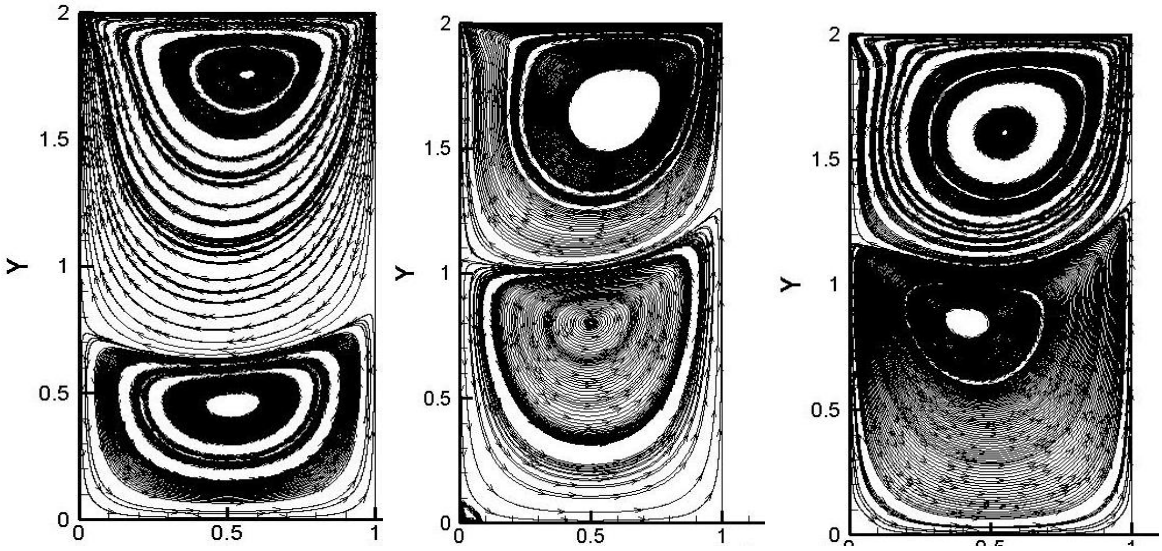

(a) (b) (c)

Fig 7. Streamline of velocity at H/L=2, (a) Re=100 (b) Re=500 (c)Re=1000

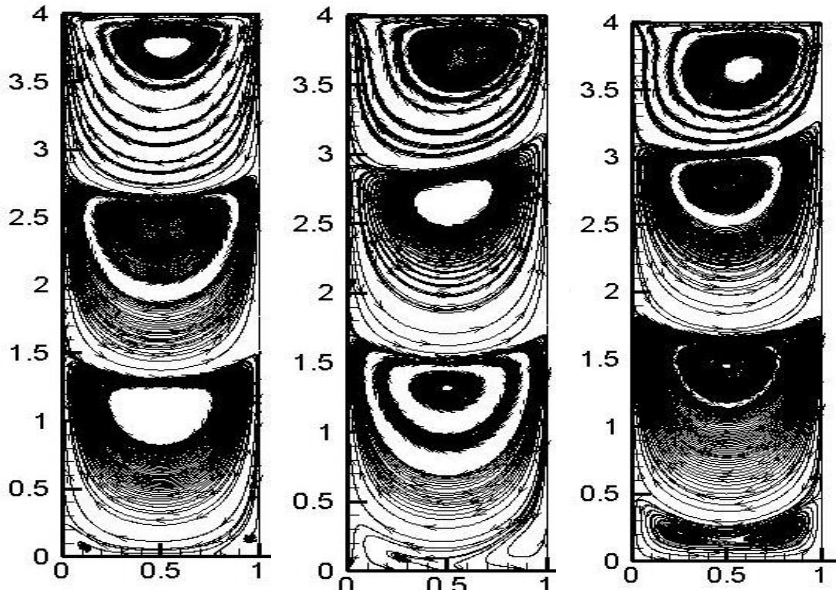

(a) (b) (c)

Fig 8. Streamline for velocity at H/L=4, (a) Re=100 (b) Re=500 (c) Re-1000

While observing the contour of streamline for different aspect ratio at different Reynolds numbers (**figure5 figure6, figure7, figure8**), it can be seen for the low aspect ratio the center of primary eddy moves right with respect to right wall cavity. For **H/L=0.5, H/L =2 and H/L =4** , At high value of Reynolds number there is a formation of secondary and ternary vortexes cause by shear force drags. On the other hand, when the aspect ratio rises above the value 1, the center of the primary eddy remains at the same place below the top lid for **Re=100,** which change by a slight displacement when the Reynolds number becomes larger. For **H/L =1** the flow distribution is mainly composed of one main vortex and two secondary vortices. The main vortex is located at the upper right corner of the center, and the secondary vortex in the lower. The secondary vortex at lower right corner is larger than the secondary vortex at the lower left corner.

We can also notice for that **Re=100** when the aspect ratio **H/L** is greater than **1**,there is a second vortex at the bottom of the cavity which is completely absent for the aspect ratio H/L=1/2 and 1. The number of these vortices increase with the increase in aspect ratio in **H/L**

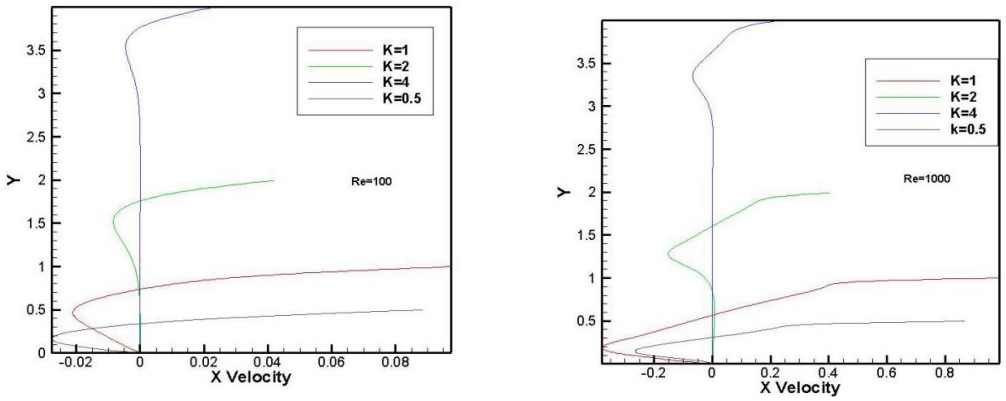

Fig 9. Computed of U-velocity profiles along a vertical line passing through the center of cavity (at X=1/2) at various ratios Re=100 and Re=1000

Figure 9 Show the U- velocity along a vertical line passing through the geometric center of different ratios (**H/L=K)** for Reynolds number equal to **100** and **1000.** We notice at the bottom wall the U peak decreases with Reynolds number although it does move towards the wall. Near the lid when the Reynolds is high there is the thin boundary layer that's shaped regardless of the ratio. The effect of Reynolds number on the U-velocity varies with ratio, dominating over larger ones and less imposing with smaller ones.

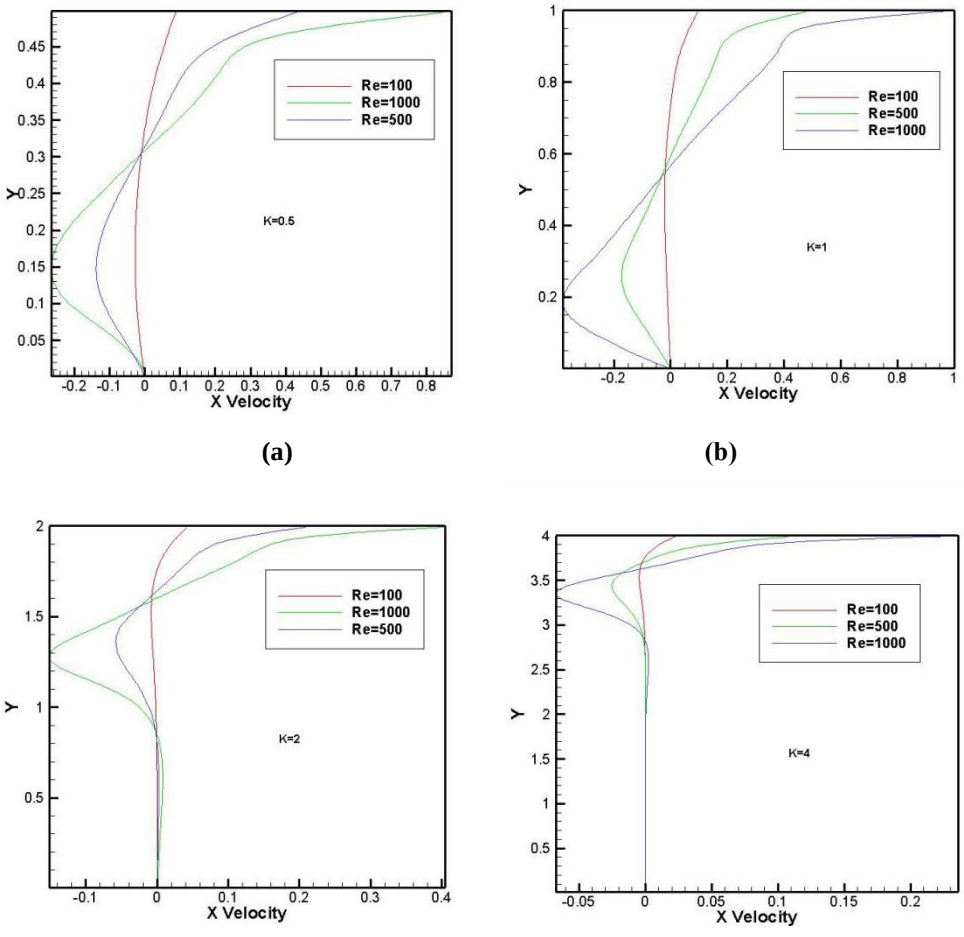

Fig 10. Computed of U-velocity profiles along a vertical passing through the geometric center of the cavity (X=1/2) at various Re, and different ratios (K=0.5, K=1, K=2, K=4)

Observing carefully at the curves of the velocity along a vertical line passing through the center of the different aspect ratio cavity for Re=1000, we clearly note the influence of the aspect ratio on the flow. More the ratio is higher more U-velocity is dominant.

It's also noted that the change of aspect of ratio causes a decrease in transmission of kinetic energy supplied by the upper wall towards the bottom of cavity.

As might be expected, Reynolds number has a strong influence on the flow, As the Reynolds number increases, the vortex layer distribution is denser and more obvious. It can be also noted that as the Reynolds number increases, the velocity profile of the cross-sectional velocity distribution will appear, the slope of the velocity profile in the flow field will gradually increase. For the low Reynolds number, the boundary layer is thicker while for low aspect ratio the boundary layer is thinner along the walls.

-Discussion on energy gradient theory

The figure 11 shows the distribution of **K** in the square at different Reynolds numbers.

We can notice that the change of streamline is more obvious as the Reynolds number is increased.The magnitude of **K** is proportional to the global Reynolds number , **K** increase with the Reynolds number. At **Re**=500 , and **Re**=1000 the **K** is more tender, not very impressive, the flow is more or less stable. On other hand at **Re**=1400 and **Re**=2000 the K becomes denser which leads to more instability of flow. The $\boldsymbol{K_{max}}$ is at the corner region between the upper wall and the left wall. According to the energy gradient theory, as the **K** increase the fluid flow become more unstable.

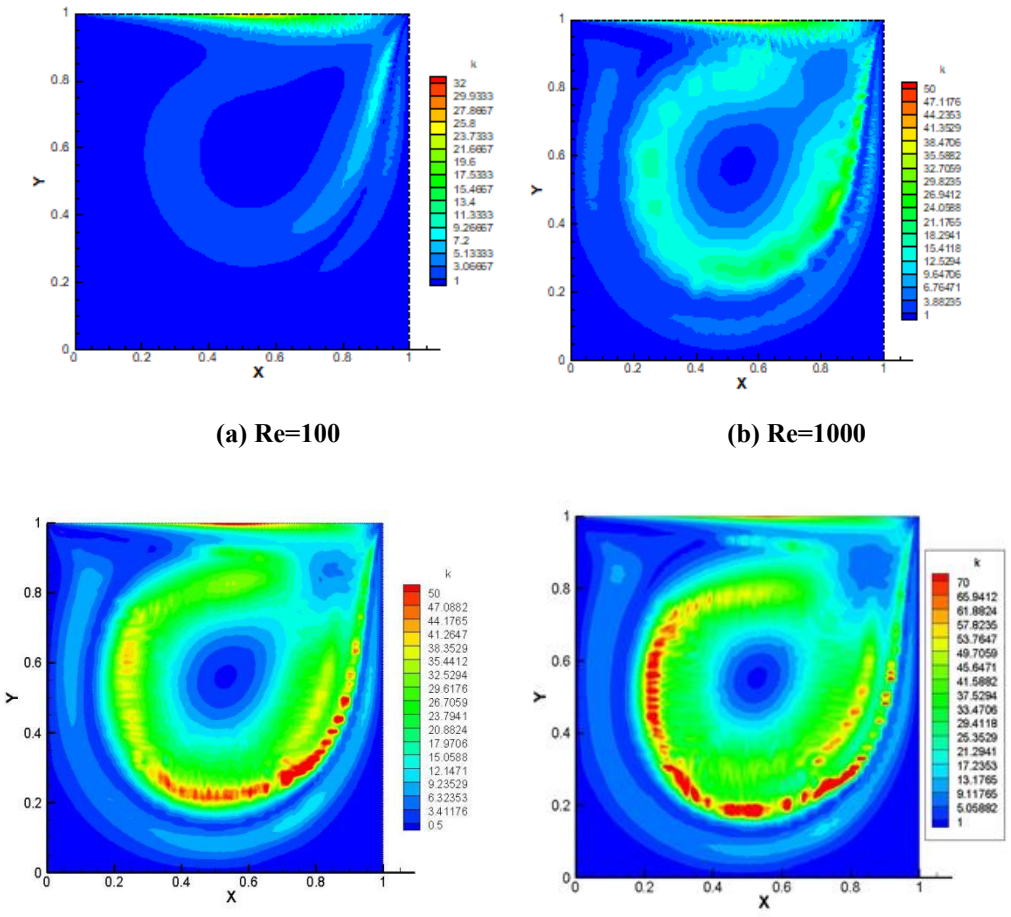

(a) Re=100 **(b) Re=1000**

(c)Re=1400 **(d) Re=2000**

Fig 11. Contour of Energy gradient function K

Figure:12 shows the distribution and comparison of a dimensionless function **K** for different **Re** at cross section **Y**=1/2.

The region of the high **K** value in the meridional plan is mainly located at the region between the circulation with both

side of square. Since the upper wall moves to the right, there is a depression in the left upper corner and an over-pressure in the upper right corner which explains the formation of the first high peak on the right. It can be noted that the dimensionless function K_{max} near the wall got his maximum.

The position with the K_{max} is the place where the oscillation and disturbance occur first. By change of the Reynolds the radical location of **K** is changed. The energy gradient function K_{max} is shifted from left toward to the over side. While knowing that the hollow in the middle would be explained by the lack of speed in the center of the vortex.

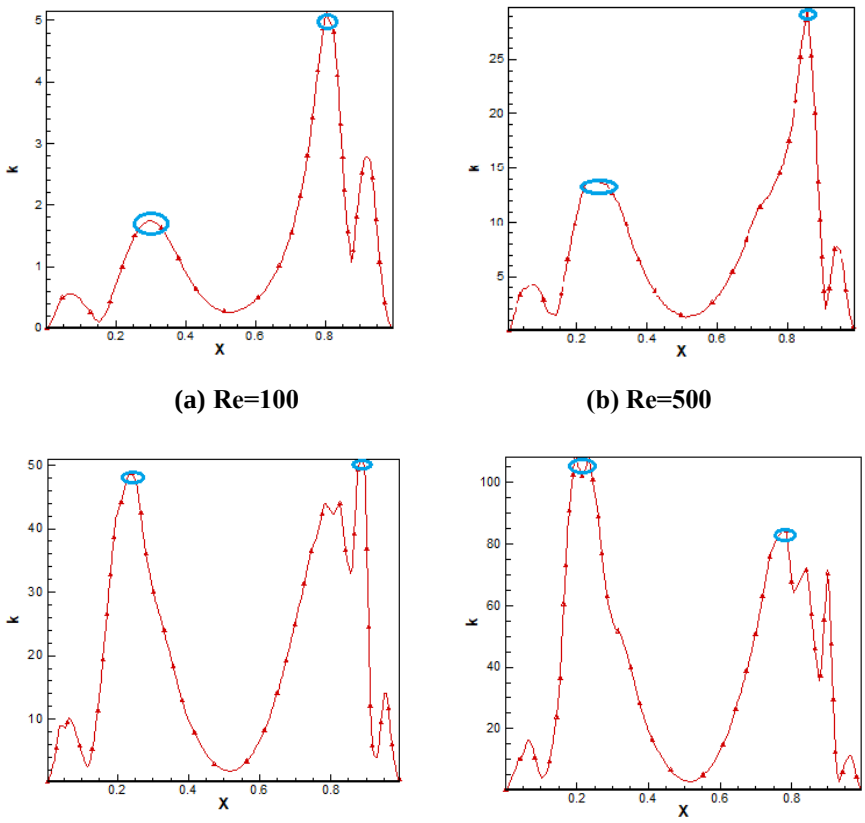

(a) Re=100 **(b) Re=500**

(c) Re=1400 **(d) Re=2000**

Fig 12. Contour of Energy gradient function K at center-line Y=1/2.

Distribution of K at differents aspect ratio H/L

Figure 13 shows the contour of the dimensionless energy gradient **K** on different ratios for the Reynolds number varying from 100 to 2000. The flow is represented by a single-stage vortex called primary vortex rotating clockwise. It should be noted that the flow remains single cell by increasing the dimensionless energy gradient **K** regardless of the ratio; However, a larger and denser primary vortex is obtained for the higher energy gradient which results in a more unstable flow. The increase of the dimensionless energy gradient **K** increases the circulation of air in a loop in the boundary layer near the walls. Then the flow becomes unsteady (starts changing from the laminar regime to the turbulent regime). It has been noticed that when the Reynolds number values are greater than 2000, a significant flow which is less and less stable settles in the cavity. As the dimensionless energy gradient **K** increases the main flow is concentrated at the walls of the cavity at the same time promoting the shearing effect which will lead to the formation of a more complex cell. The dimensionless energy gradient increase leads to a turbulent regime.

On the Reynolds range at which new flow states appears a bifurcation of solutions takes place. We have seen that the field of influence of the **K** energy gradient on the flow was restricted to the amplitude of the modes, the distribution of energy, but had little impact on the structure and dynamics of the flow.It has been noticed that the parameter for establishing a classification of the various cavity flows, according to observations in temporal means, was the ratio **H/L.**

In short, we can note that the magnitude of dimensionless energy gradient **K** is proportional to the global Reynolds number, the more it increases the flow becomes unstable independently of the ratio.

H/L=0.5

Re=100

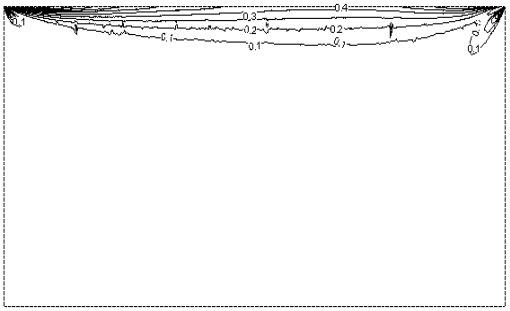

Re=500

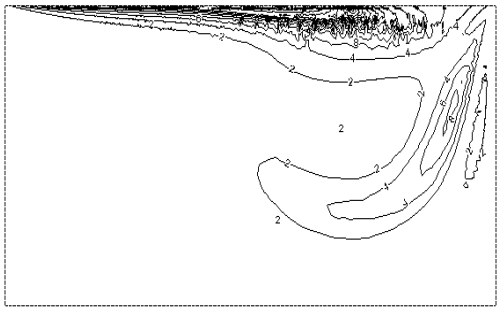

Re=1000

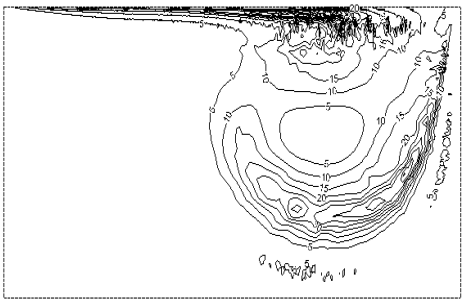

Re=2000

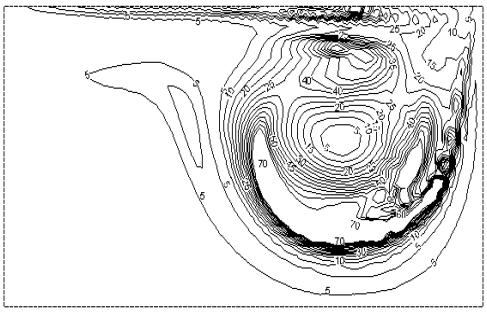

H/L=1

Re=100

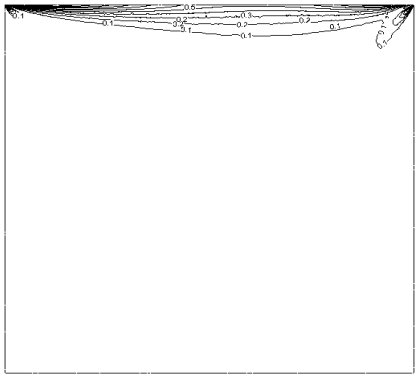

Re=500

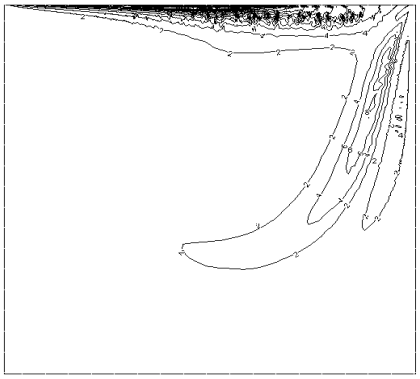

Re=1000

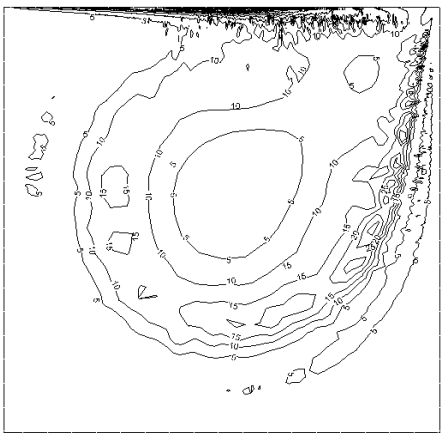

Re=2000

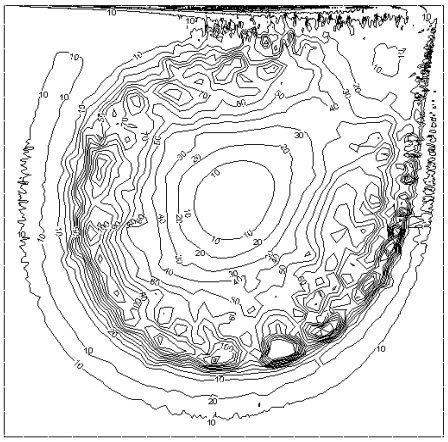

H/L=2

Re=100

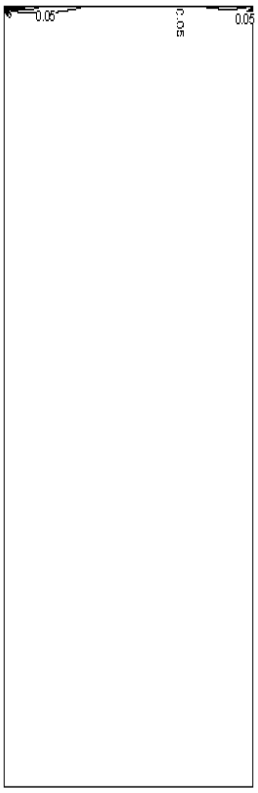

Re=500

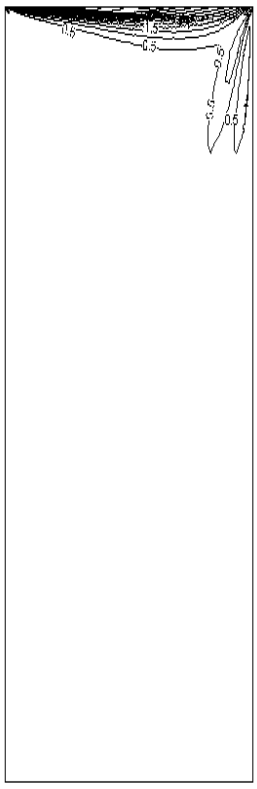

Re=1000

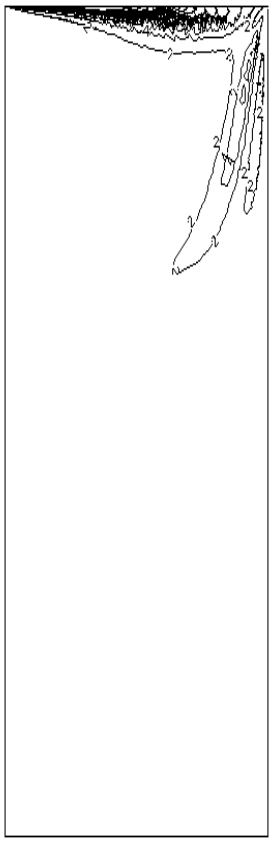

Re=2000

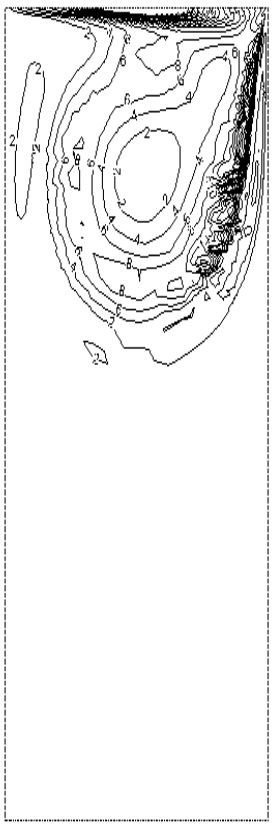

H/L=4

Re=100 **Re=500**

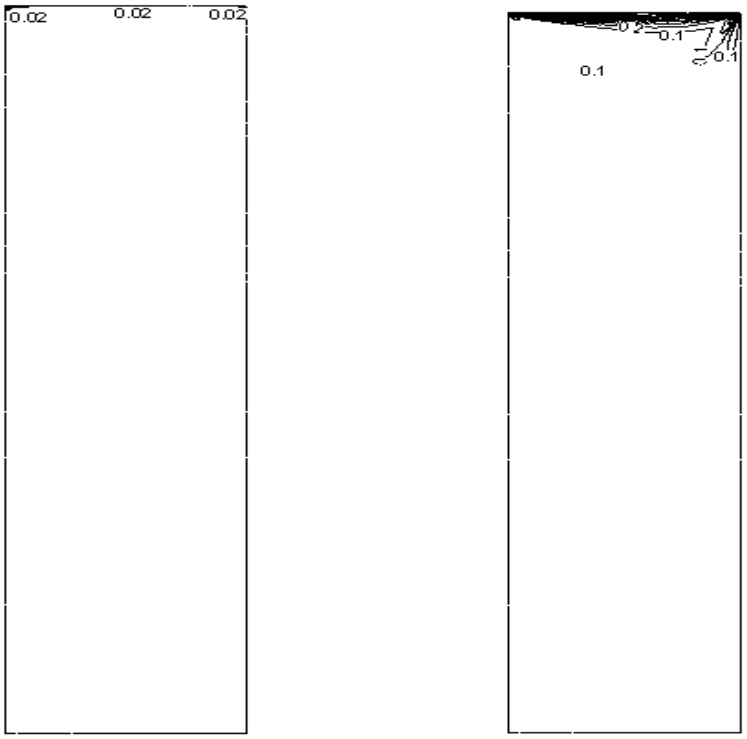

Re=1000 **Re=2000**

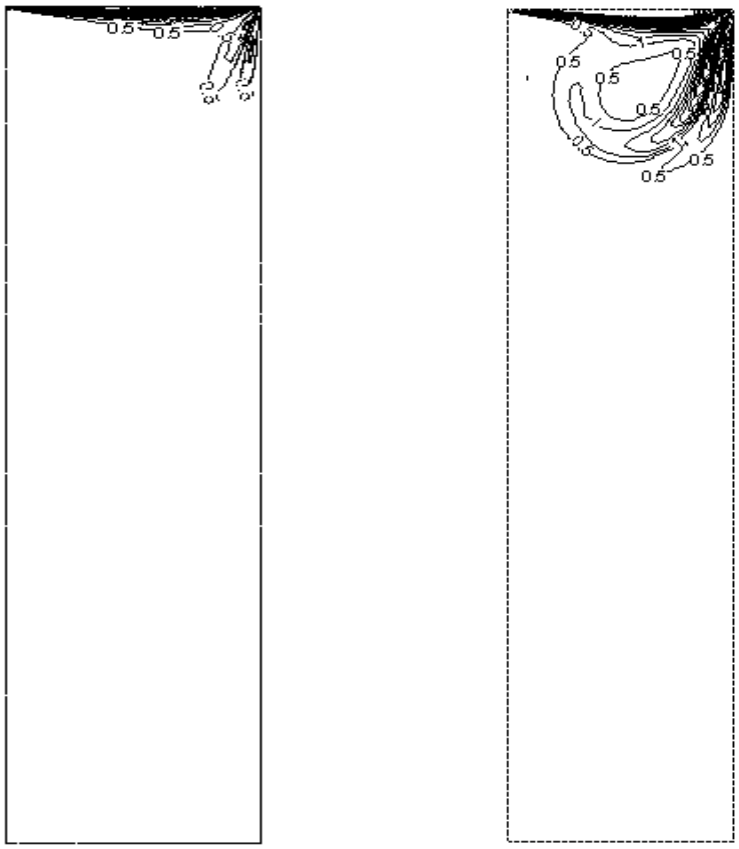

Fig 13: Contour of K at different ratio

5. CONCLUSION

Computational fluid dynamics (CFD) simulations are performed for laminar incompressible fluid flow in lid driven cavity. This paper presents firstly the numerical investigation of flow for various Reynolds numbers and aspect ratios to understand the effects of the Reynolds number and aspect ratio in the flow, secondly the analyze of the flow instability using energy gradient theory. The results show that:

- The main vortex behavior is totally dependent on the Reynolds number as well as the aspect ratio.

-The component ratio **H/L** of the cavity may be interpreted in parallel with the Reynolds number, as a second bifurcation parameter representing the field of flow.

- It was noted also that as the Reynolds number increases, the velocity profile of the cross-sectional velocity distribution will appear, the gradient of the velocity profile in the flow field will progressively increase.

- The higher the Reynolds number is, the bigger **K** (energy gradient) value become, which proves that the magnitude of **K** is proportional to the global Reynolds number, it can be considered to be the local Reynolds number.

- The stability or instability in the lid driven cavity is highly dependent on Reynolds number and at the same time on the gradient energy, can only be controlled by regulating the Reynolds number hence the **K** (the distribution of the energy gradient function).

- Value of energy gradient function **K** at the corner eddy and re-circulation zone is significantly higher and therefore, these regions are candidate of the onset instability in a lid driven flow.

- Regardless of the ratio, the increase in the energy gradient easily accelerates the flow in the cavity which leads to an intensification of the air in a loop in the boundary layer near the walls.

In view of the above it can be concluded that: like in Taylor-Couette flow; plane Couette; plane Poiseuille and pipe Poiseuille, Energy gradient method has also strong capability to study of flow field stability in Lid driven cavity.

REFERENCES

[1] **Botella and Peyret** Benchmark spectral results on the lid-driven cavity flow. Computer and fluid 1998; 27:421-433.

[2] **Rubin and Khosla** Navier -Stokes calculations with a strongly implicit method. Computer and fluid.

[3] **U Ghia, K. N. Ghia, and C. T. Shin** High-Re solutions for Incompressible flow Using the Navier-Stokes Equations and a Multigrid Method. Journal of computational physics 48,387-411(1982).

[4] **Li M, Tang T, Fornberg B.** A compact fourth-order finite difference scheme for the steady incompressible Navier-Stokes Equation. International journal for numerical Method in Fluid. 1995; 20:1137-1151.

[5] **Carlos H. M, Roberta S., Luciano K.A**., The Lid-driven cavity square cavity flow: Numerical solution with a 1024*1024 Grid.

[6] **S. HOU, Q. Zou, S. Chen, G. Doolen, A. Cogley**, Simulation of cavity flows by lattice Boltzmann method. J. Comput. Phys. 118(1995) 329-347.

[7] **Ch. H. Bruneau, M. Saad,** the 2D lid-driven cavity problem revised, Computers and Fluids 35, 2006

[8] **E. Erturk, T. C. Corke and C Gokcol**, Numerical solutions of 1D steady incompressible driven cavity flow at high Reynolds numbers; Int. J. Numer. Meth. Fluid 2005; 48: 747-774.

[9] **Ercan Erturk**, Discussion on driven cavity flows, Int. J. Numer. Meth. Fluid 2009; 60: 275-294.

[10] **M. Taghilou,** Simulation of lid driven cavity flow at different aspect ratios using relaxation time lattice Boltzmann method, Int. J. Eng. 26(2012) 1471-1478.

[11] **Dou H S** 2006 Mechanism of flow instability and transition to turbulence. International Journal of Non-Linear Mechanics. **41** 512-517.

[12] **Dou H S** 2011 Physics of flow instability and turbulent transition in shear flow. International Journal of Physical Science. **6(6)** 1411-1425.

[13] **Dou H S, Khoo B C, Yeo K S** 2008 Instability of Taylor – Couette flow between concentric rotating cylinders International. Journal of Thermal Sciences. **47** 1422-35

[14] **Dou H S, Khoo B C, Tsai H M** 2010 Determining of the critical condition for turbulent transition in a full-developed annulus flow. Journal of Petroleum Science and Engineering. **73** 41-47

[15] **Dou H S, Khoo B C** 2011 Theory and prediction of turbulent transition International. Journal of Fluid Machinery & Systems. **4** 114-132

[16] **Dou H S** Energy gradient theory of hydrodynamic instability, The third International Conference on Nonlinear Science, 30 June-2 July 2004

[17] **Dou H S, Khoo B C** 2011Investigation of turbulent transition in plane Couette flows Using Energy Gradient Method, Advances in Appl. Math. And Mech. 3(2), 165-180

[18] **J.R. Koseff, R.L. Street** the Lid- driven cavity flow: A synthesis of qualitative and quantitative Observation.

[19] **A. M. Grillet, E. S. G. Shaqfeh**, and **B. Khomami.** Observations of elastic instabilities in lid-driven cavity flow. J. Non-Newtonian Fluid Mech., 94:15–35, 2000.

[20] **M. M. Gupta, R. P. Manohar**, and **B. Noble**. Nature of viscous flows near sharp corners. Comp. Fluids, 9:379–388, 1981.

[21] **F. G¨urcan.** Streamline topologies in Stokes flow within lid-driven cavities. Theor. Comput. Fluid. Dyn., 17:19–30, 2003.

[22] **F. G¨urcan** and **H. Bilgil.** Bifurcations and eddy genesis of Stokes flow within a sectorial cavity. Eur. J. Mech. B/Fluids, 39:42–51, May 2013. ISSN 0997-7546.

[23] **K. Gustafson** and **K. Halasi.** Cavity flow dynamics at higher Reynolds number and higher aspect ratio. J. Comput. Phys., 70:271–283, 1987.

[24] **J. M. Floryan and L. Czechowski**. On the numerical treatment of corner singularity in the vorticity field. J. Comput. Phys., 118:222–228, 1995.

[25] **A. Fortin, M. Jardak, J. Gervais, and R. Pierre**. Localization of Hopf bifurcation in fluid flow problems. Int. J. Numer. Methods Fluids, 24:1185–1210, 1997.

[26] **L. Fuchs and N. Tillmark**. Numerical and experimental study of driven flow in a polar cavity. Int. J. Num. Meth. Fluids, 5:311–329, 1985.

[27] **S. Garcia.** The lid-driven square cavity flow: From stationary to time periodic and chaotic. Commun. Comput. Phys., 2:900–932, 2007.

[28] **B. B. Gogoi. Global** 2D stability analysis of the cross lid-driven cavity flow with a streamfunction-vorticity approach. Int. J. Comp. Meth. Eng. Sci. Mech., 17(4): 253–273, 2016.